Article

Journal of
Nanoscience and Nanotechnology
Vol. 15, 1297–1303, 2015
www.aspbs.com/jnn

Direct Tailoring the Si Substrate for Antireflection via Random Nanohole Nanoimprint

Tangyou Sun[1], Zhimou Xu[1,*], Haifeng Xu[1], Wenning Zhao[1], Xinghui Wu[1], Sisi Liu[1], Zhichao Ma[1], Zheng Zhang[1], Jian He[1], Shiyuan Liu[2], and Jing Peng[3]

[1] *Wuhan National Laboratory for Optoelectronics, School of Optical and Electronic Information, Huazhong University of Science and Technology, Wuhan 430074, China*
[2] *State Key Laboratory of Digital Manufacturing Equipment and Technology, Huazhong University of Science and Technology, Wuhan 430074, China*
[3] *College of Sciences, Wuhan University of Science and Technology, Wuhan 430081, China*

In this paper, a 2 inch random nanohole Si template with hole diameter of 36–97 nm is employed for direct tailoring the Si substrate for antireflection. The random nanohole Si template is fabricated from the natural self-organization process and can be used repeatedly in nanoimprint lithography (NIL). The surface roughness induced from the nanohole structured surface enhanced the anti-adhesion property (contact angle of 128°) of the Si template for high accuracy soft mold replication. The random nanohole structured polymer/Si substrate has a surface fluctuation of ∼3 nm, which ensures a uniform and effective pattern transfer from resist to substrate. The reflectivity of the random nanohole structured Si substrate decreases from around 34% to less than 5% with the hole aspect ratio within 3.0 in the wavelength region of 400–800 nm. This method is simple, cheap, repeatable in large area and compatible with the high volume production lines.

Keywords: Subwavelength Structures, Antireflection, Random Nanohole, Nanoimprint Lithography.

1. INTRODUCTION

In order to suppress the undesired Fresnel reflections, an additional layer with a thickness of quarter-wavelength is usually employed as the antireflection coating (ARC). However, the ARC obtained in this way encounters two major problems: (1) the reflectance only reaches the minimum at a single wavelength (λ_{min}) and gradually increases as the wavelength deviates from λ_{min}; (2) the adhesion and the thermal stability of the ARC are generally unsatisfactory due to the mismatch of material properties between the ARC and corresponding substrate.[1] Subwavelength structures (SWSs), inspired by moth-eye corneas which comprise of periodic arrays of protuberance,[2] have been demonstrated as an alternative to attain superior antireflection performances, including broad-band working ranges,[3] omnidirectionality[4] and polarization insensitivity.[1] Despite the excellent antireflection properties, the SWSs are usually fabricated directly or indirectly through the tedious and time-consuming focused ion beam (FIB) or electron beam lithography (EBL) methods,[5–9] which conversely limits the potential application of SWSs.

Since the anodic aluminum oxide (AAO) method was proposed by Masuda and Fukuda in 1995,[10] the high density honeycombed sub-100 nm nanohole structures of AAOs have been widely used to prepare the SWSs for various optical and optoelectronic devices. The commercial value outstands in the widespread use of solar cells,[11,12] light-emitting diodes (LEDs),[13,14] lenses[15] and transparent polymer,[16] etc. Among all these applications adopting AAOs, the pattern transfer process is of great importance and hardness due to the requirements for low dimension and large area uniformity. In most cases, a simple single imprint process is performed on the target sample (a thermal or UV curable polymer) for transferring the nanostructures from AAO.[12–16] However, the alumina itself is essentially friable and can be used with limited times under the high pressure imprinting. Furthermore, little attention is paid to the direct patterning of the thermal and UV stable semiconductor materials, like Si, SiO_2 and gallium nitride (GaN), etc. As a matter of fact, the SWSs

*Author to whom correspondence should be addressed.

nanofabrication of these substrates is routinely practiced on the optical and optoelectronic devices such as Si-based solar cells and LEDs.[17–21] In the previous few researches, Kanamori et al. proposed a direct Si surface patterning process by using the AAO as an etching mask.[20,21] However, the mask layer used in this way must be removed at any single fabrication cycle. Thus it fails to meet the repeatable requirement. Although Zhou et al. demonstrated a soft UV nanoimprint lithography (SUNIL) combined with AAO process to fabricate the nanohole structured LED for a higher external quantum efficiency,[19] the nanopillar arrays will have a nonuniform pattern depth due to the dimension-related filling speed of the polymer. Besides, since NIL is a 1:1 pattern transfer process, the nonflat surface morphology of AAO will be transferred to the patterned resist to gain a nonuniform residual resist thickness, thus, the information of the nanostructure will be immersed in such surface nonflatness in subsequent process of residual resist removal.[22] In this work, a self-organized random nanohole template is employed as the initial template of NIL for direct tailoring the Si substrates. A three-step pattern transfer process, namely the soft mold replication, the SUNIL by using the soft mold and the inductive coupled plasma (ICP) dry etching, is applied for transferring the nanostructures. Detailed information at any single step is studied, including the anti-adhesion property, the surface flatness of patterned polymer, the influence of the aspect ratio and the corresponding antireflection performance.

2. EXPERIMENTAL DETAILS

2.1. Preparation of the Random Nanohole Si Mold

The random nanohole Si mold is fabricated through the well-known two-step anodization process. The detailed fabrication method has been described in previous work of our group.[22] As shown in Figure 1, the as-prepared random nanohole Si mold has a pore diameter of 36–97 nm and a pore depth of ∼84 nm.

2.2. Three-Step Pattern Transfer Process

Replication of the soft mold from initial template is necessary for NIL, while the current NIL techniques with rigid templates rely strongly on the substrate flatness and the production atmosphere. These facts hinder the integration of NIL into high volume production lines.[23] In our experiment, pressure-assisted molding (PAM) technique is applied to ensure the complete filling of the nanostructures.[23] Figure 2 shows the overall patterning process of the three-step pattern transfer process. The soft mold is fabricated by pressing the relatively hard initial template against the IPS (a thermal-curable polymer film, developed by Obducat AB) through thermal NIL at the temperature of 155 °C and pressure of 40 bar respectively. The IPS soft mold is obtained after demolding at room temperature. Soft UV-NIL is performed on Eitre3 Nano

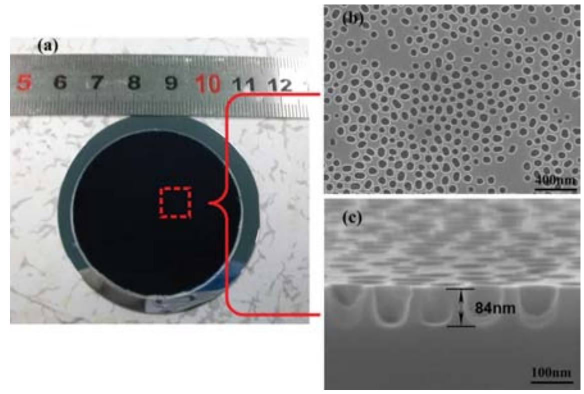

Figure 1. Scanning electron microscope (SEM) micrographs of the prepared random nanohole Si mold: (a) Photograph of the two-inch random nanohole Si mold. (b) The surface image. (c) The corresponding cross-sectional image.

Imprinter. The nanoimprint pressure is 20 bar and hold time for UV exposure of 60 seconds. Before soft UV-NIL, the substrate is spin-coated with TU2 resist (a UV-curable resist, developed by Obducat AB), then baked at 95 °C for 3 minutes. After soft UV-NIL, ICP dry etching is applied for substrate patterning. The energy for polymerization of TU2 resist and the energy density of UV source are 22.5 mJ/cm^2 and 35 mW/cm^2, respectively. The detailed values for residual resist removal and subsequent Si etching can be seen in our previous works.[22,24]

2.3. Characterizations

The contact angle of the water on the initial Si mold is measured by SL200B (KINO INDUSTRY Co., Ltd., USA). The initial template, the imprinted patterns on resist and the random nanohole structured Si are measured by SEM (Nova NanoSEM450, FEI). The surface nonflatness is investigated by atomic force microscope (AFM, NanoScope MultiMode, VEECO). Reflectivity measurements are performed with a JASCO V-670 UV-vis spectrometer equipped with an integral sphere.

3. RESULTS AND DISCUSSION

A surface treatment was performed by immerging the random nanohole Si mold into a 0.6 mmol/mL 1 H, 1 H, 2 H, 2 H perfluorodecyltrichlorosilane (FDTS)/isooctane solution for 10 min for anti-adhesion.[25] Then it was cleaned with isooctane, acetone, IPA and water, and at last blown dried. The photo, recorded with a CCD camera, of a droplet on the as-prepared random nanohole Si mold is shown in Figure 3. The water contact angle of the as-treated random nanohole Si mold is 128°, which is rather higher than the commonly practiced circumstance on the SiO_2 mold with a F_{13}-OTCS (Tridecafluoro-1,1,2,2-Tetrahydrooctyl Trichlorosilane) deposition of ∼113°,[26] serving as a good initial mold for the subsequent NIL

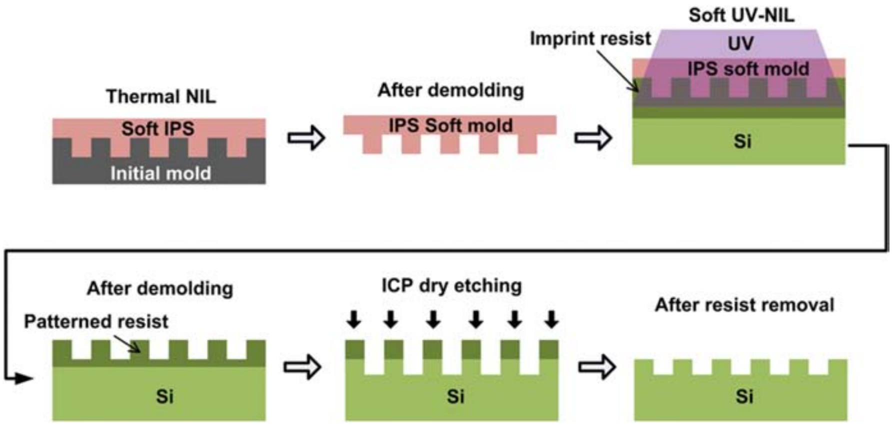

Figure 2. The process flow of the three-step pattern transfer process.

process. The high hydrophobicity of the as-treated random nanohole Si mold is believed to be partly caused by the air trapped in the nanoholes, which can be explained according to Cassie and Baxter's theory.[27] Specifically, Wenzel indicates that the cosine of the contact angle of a droplet on a rough surface is proportional to the roughness factor:[28]

$$\cos(\theta_{\text{rough}}) = \gamma \cos(\theta_{\text{smooth}}) \tag{1}$$

Where θ_{rough} and θ_{smooth} represent the contact angles a fluid establishes on rough and smooth surfaces respectively, and γ is the average roughness ratio, defined as the factor by which roughness increases the solid–liquid interfacial area.

Figure 4 is the IPS nanorod array obtained through the as-described thermal NIL process. As shown, the distribution of the nanorod array is consistent with that of the initial mold in Figure 1(b), which reveals, in reverse, the excellent hydrophobicity of the as-treated random nanohole Si mold. The nanorod arrays are commonly used in the antireflection field. According to the Mie and Rayleigh scattering theory, light can't recognize any medium that is smaller than λ/n.[29] Therefore, light can't recognize the nanopore structures when its wavelength (λ/n) is longer than the product of pore dimension and the refractive index of corresponding substrate. The patterned layer will be considered as a uniform layer with a lower refractive index, which thus can be used as an antireflection film to improve the corresponding efficiency. The effective refractive index (n_{eff}) gradient of the nanorod array can be estimated in the equation:[30]

$$n_{\text{eff}}(h) = \{f(h)n_{\text{sub}}^{q} + [1 - f(h)]n_{\text{air}}^{q}\}^{1/q} \tag{2}$$

Where q is 2/3, n_{sub} and n_{air} are respectively the refractive indices of the substrate and air and $f(h)$ is the fill factor, which is defined as the area ratio of nanorod array to the total substrate surface at height (h) and can be obtained by the SEM images. According to this equation, it is reported that increasing the edge tilt of the nanorod array will lead to more grading in n_{eff} from air to the substrate and thus a more excellent antireflection performance.[1, 15, 16, 20, 21, 31–33] To this point of view, it is convenient to direct tailoring the surface of a polymer for high performance antireflection

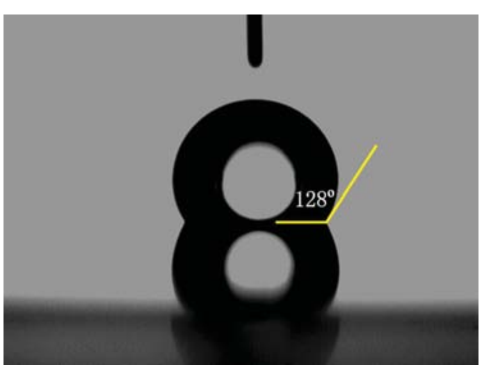

Figure 3. Contact angle measurement on the anti-adhesion treated random nanohole Si surface.

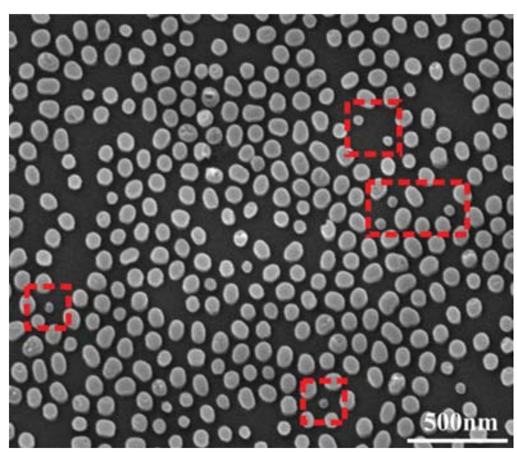

Figure 4. A representative SEM image of the soft IPS mold created from random nanohole Si master.

via a V-shape nanohole initial mold and a single step NIL process.[15, 16] While in three-step pattern transfer process, as the soft mold for NIL, the V-shape nanorod arrays are too weak to realize a good pattern transfer. In our experiments, the pillar-like nanorod array is adopted. The smallest diameter of the nanorods (indicated in the red dash line boxes) in Figure 4 is $\sim$35 nm, thus the corresponding aspect ratio will be $\sim$2.4 since the depth of the nanoholes is $\sim$84 nm. As a matter of fact, this aspect ratio is of great importance in NIL. To fabricate nanorod array for the optimum SUNIL experimentally, we have to consider the effect of the nanorod array height on the mechanical stability carefully. If the aspect ratio (L/D; length/base diameter of paraboloid) of the nanorod array increases above a certain critical value, a number of nanorod arrays may locally adhere to each other to form bundles. For example, local adhesion of PMMA nanorod array has been respectively observed at 3.0 and 4.4 ratio, and for an even higher aspect ratio, even larger bundles have been formed.[34, 35] Obviously, this critical value of NIL must be much lower than that of the adhesion to keep a better mechanical stability under the high pressure in NIL. The aspect ratio will be shown to play an important role in subsequent SUNIL process.

Different from NIL by using uniform mold, the random nanohole NIL has its unique features. Figure 5(a) is the surface of patterned resist on Si. It can be observed that some of the holes are stuffed by the IPS nanorods in Figure 5(a). This is because of the effect of as-described aspect ratio. Before UV exposure, the IPS nanorods are all pressed in to the TU2 resist. But at this stage, due to the flat soft SUNIL, every nanorod shares the same amount of pressure and the soft mold deformation will not be induced at such a low aspect ratio ($<$2.4) of nanorods.[22] It should be mentioned that the flat IPS soft mold is obtained due to the following reasons:

(1) the PAM technique is applied to ensure the complete filling of the nanostructures,[23] thus the nonuniform resulting from the dimension-related filling speed of polymer will not be induced;[26]

(2) because the NIL is a 1:1 pattern transfer process, the flat surface of the initial nanohole Si mold can be transferred to IPS to form a smooth substrate of the soft mold;[22]

(3) the uniform depths of nanorods are realized due to the high resolution ICP dry etching, which means that the surfaces of the nanorods are in the same plane.

After UV exposure, the IPS soft mold is torn off from the resist surface. In this step, each nanorod under goes the adhesion force between the nanorod itself and UV curable resist. The nanorod with less mechanical strength (or lower than the critical aspect ratio) will break and remain in the resist rather than maintain on the surface of the soft mold. This critical aspect ratio can be calculated from the SEM image. As shown in Figure 5(b), the largest diameter of the nanorods (indicated in the red dash line boxes) is $\sim$43 nm, thus the critical aspect ratio is $\sim$2.0. That means the nanorods with the aspect ratio higher than 2.0 will be trapped in the TU2 resist, and thus the corresponding features will be lost. Although one can control the depth of the nanorod by using a short time ICP etching in the process of initial mold fabrication, the patterned resist with a lower aspect ratio of nanohole is not a good etching mask for subsequent substrate patterning.[24, 36] Besides, it is inspired to improve the regularity of the nanohole to achieve a same aspect ratio for all nanorods, but the random nanohole distribution still can't be avoided due to the effect of the aluminum grain in the anodization process.[37]

To date, the nanostructured surface has been widely used as an antireflection layer for its effect on the reduction of refractive index of the corresponding native material.[29, 38] Beside the remarkable optical properties, the surface tailored with sub-wavelength structures exhibits improved mechanical strength, thermal stability and durability as compared to the thin-film counterpart.[17] Benefiting from the flat IPS soft mold, after SUNIL, the random nanohole patterned resist layer is a good mask layer for subsequent ICP dry etching.[22] As shown in Figure 6(a), the vertical sidewall and the uniform hole depth of $\sim$83 nm can be observed, which is consistent with that of the initial random nanohole Si mold. Figure 6(b) is the surface image of the random nanohole patterned resist layer. The nonflatness of the surface is tested to be less than 3 nm.

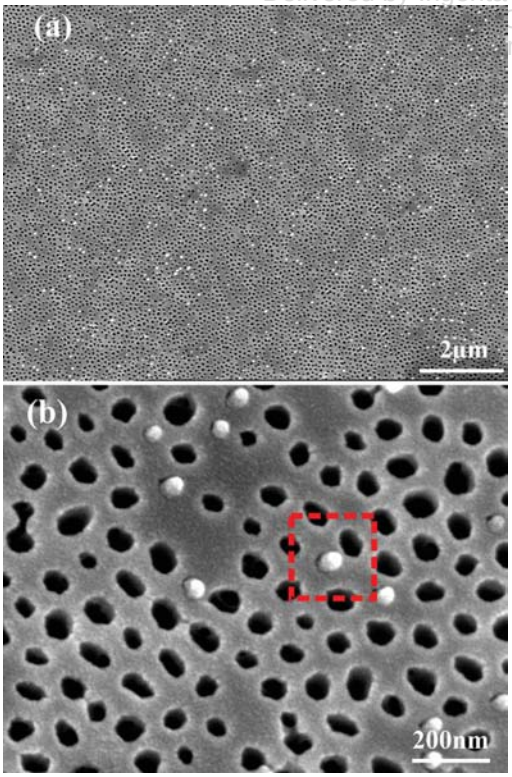

Figure 5. (a) SEM image of imprinted patterns. (b) The enlarged magnification image showing the detached IPS nanorods.

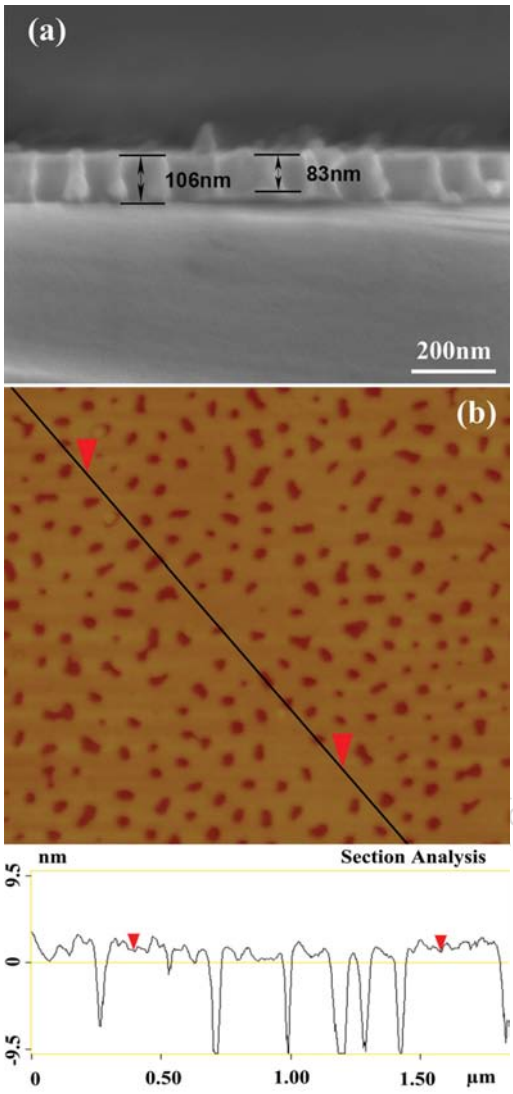

Figure 6. (a) Cross-sectional image of imprinted resist. (b) An AFM image of the patterned resist surface.

Thus because of the flat surface, the vertical sidewall as well as the uniform pattern depth, the effective pattern depth is almost the same as that of the initial random nanohole mold after removing the residual resist via dry etching. A O_2 ICP dry etching is applied to remove the residual resist after Si etching. The as-fabricated Si surface is shown in Figure 7. The smallest diameter of the random nanoholes in Figure 7(a) is ∼57 nm which is larger than that of the initial random nanohole Si mold. This difference is due to the following reasons: (1) the nanoholes with diameter less than 43 nm vanishes on account of being blocked with IPS nanorods; (2) the etching selectivity of TU2 resist to Si is not large enough, so the lateral etching will lead to a larger lateral dimension. The random nanohole depth can be observed from

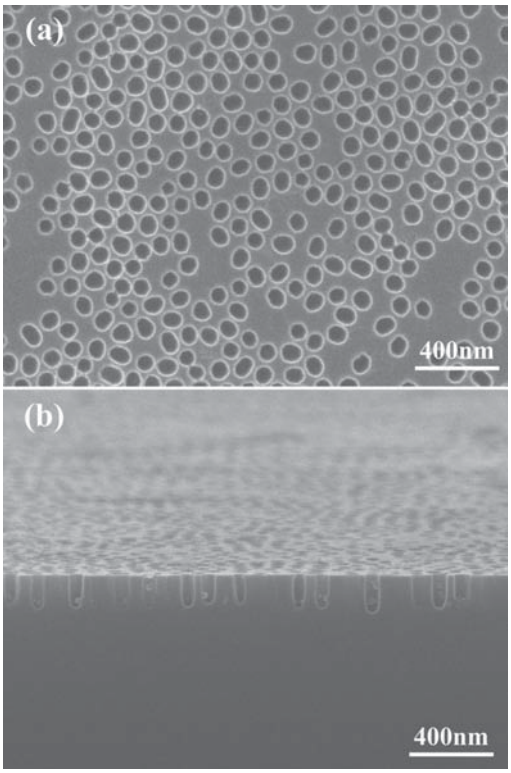

Figure 7. SEM images of the random nanohole structured Si after dry etching and resist removal: (a) Surface image. (b) Cross-sectional image.

Figure 7(b). The average hole depth of the as-fabricated random nanoholes is ∼171 nm, thus the average aspect ratio must be less than 3. The reflectivity of the random nanohole structured Si is shown in Figure 8. In the wavelength region from 400 to 800 nm, the reflectivity of the Si surface decreases from around 34% to less than 5%. Actually, similar literature has illustrated that the reflectivity of the SWS surface of Si will have a lower value of ∼1.6% with a larger aspect ratio of ∼12.[21] In this regards, our three mask layer NIL process is of great use for the high aspect ratio nanostructure fabrication by improving the corresponding etching selectivity.[24] Besides, it has been reported that the high antireflection performance of the SWS surface can be realized by the *V*-shape nanohole structure with a low aspect ratio.[11, 20, 33] Anyway, the proposed three-step pattern transfer process is demonstrated a success for direct tailoring of the substrate surface for high performance antireflection property. A small fluctuation of about 2%–3% is observed at the wavelength region from 445 to 495 nm in Figure 8. This fluctuation has never been reported anywhere and is believed to be associated with the random nanohole distribution. Due to the random nanohole distribution, parts of the Si surface will not be patterned with nanoholes. The non-patterned parts have a lateral dimension of several hundred nanometers and cannot be recognized as the SWSs. Consequently, the non-patterned

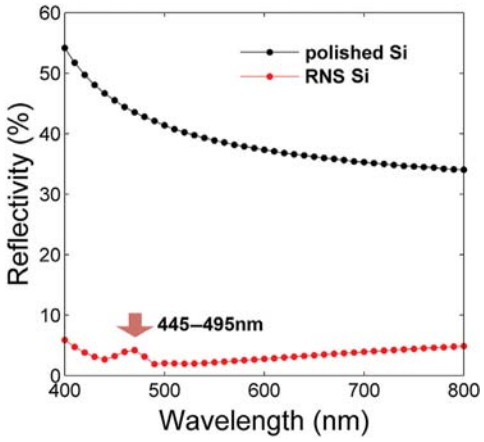

Figure 8. The reflectivity of the random nanohole structured (RNS) Si as a function of wavelength.

parts will have higher refractive indexes than the surrounding parts and thus may cause the fluctuation in Figure 8. Although the exact reason for the fluctuation is not clear enough at present, the random nanohole structure is of great use in the field of blue LED, where the nanostructure patterned sapphire substrate is required for improving the internal quantum efficiency and a higher reflectivity is needed for a higher external quantum efficiency.[39, 40]

The proposed method demonstrates a success for direct tailoring of the Si substrate. The high hydrophobicity of the random nanohole structure is of great use in outdoor self-clean filed.[11] Further pattern transfer via the random nanohole structured thin film can be repeatedly applied on conventional semiconductor materials for a higher antireflection performance of corresponding devices. As a matter of fact, the regularity of the nanohole Si template can be well controlled with the thicker aluminum film method or the free-standing alumina mask layer technique.[41, 42] Besides, AAOs with interpore distance ranging from 5 nm to 1.2 μm have been reported,[43–46] and AAOs nanostructure used as photonic crystal have been studied.[47] It is believed that our method will broaden the use of AAO and NIL and find extensive applications in optoelectronic device mass production field.

4. CONCLUSIONS

In summary, we propose the three-step pattern transfer process for substrates direct tailoring via a random nanohole Si initial mold. The key process of pattern transfer by three-step pattern transfer process is studied in details, including the soft mold replication, the SUNIL by using soft IPS mold, the dry etching for substrate patterning and the feature size loss in every step. The random nanohole structured surfaces present an excellent antireflection performance comparing with that of flat surfaces. In the wavelength region from 400 to 800 nm, the reflectivity of the random nanohole structured Si surface decreases from around 34% to less than 5%. The three-step pattern transfer process using the random nanohole Si mold is original and demonstrates a success in SWS fabrication. This method is simple, cheap and repeatable in large area, thus may find its application in optical and/or optoelectronic devices, especially for the improvement of corresponding efficiency of LEDs and solar cells.

Acknowledgments: Thanks Xiaoping Li engineer in the Center of Micro-Fabrication and Characterization (CMFC) of WNLO for the support in ICP dry etching. Thanks to the facility support of the Center for Nanoscale Characterization and Devices, Wuhan National Laboratory for Optoelectronics (WNLO). This work is supported in part by the National Natural Science Foundation of China (Grant No. 61076042), the Special Project on Development of National Key Scientific Instruments and Equipment of China (Grant No. 2011YQ16000205), and the National High Technology R&D Program (863 Program) of China (Grant No. 2011AA03A106).

References and Notes

1. Y.-R. Lin, K. Y. Lai, H.-P. Wang, and J.-H. He, *Nanoscale* 2, 2765 (**2010**).
2. P. Clapham and M. Hutley, *Nature* 244, 281 (**1973**).
3. C.-H. Sun, P. Jiang, and B. Jiang, *Appl. Phys. Lett.* 92, 061112 (**2008**).
4. Y.-F. Huang, S. Chattopadhyay, Y.-J. Jen, C.-Y. Peng, T.-A. Liu, Y.-K. Hsu, C.-L. Pan, H.-C. Lo, C.-H. Hsu, and Y.-H. Chang, *Nat. Nanotechnol.* 2, 770 (**2007**).
5. J. Y. Chen and K. W. Sun, *Thin Solid Films* 519, 5194 (**2011**).
6. Q. Chen, G. Hubbard, P. A. Shields, C. Liu, D. W. E. Allsopp, W. N. Wang, and S. Abbott, *Appl. Phys. Lett.* 94, 263118 (**2009**).
7. X. Badel, R. Rajendra Kumar, P. Kleimann, and J. Linnros, *Superlattice. Microst.* 36, 245 (**2004**).
8. X. Zhang, W. Que, and T. Gao, *J. Nanosci. Nanotechnol.* 12, 6538 (**2012**).
9. S. Ng, H. Wong, H. Lau, and C. Leung, *J. Nanosci. Nanotechnol.* 12, 6315 (**2012**).
10. H. Masuda and K. Fukuda, *Science* 268, 1466 (**1995**).
11. J. Son, L. Kumar Verma, A. J. Danner, C. Singh Bhatia, and H. Yang, *Opt. Express* 19, A35 (**2011**).
12. J. H. Lee, D. W. Kim, H. Jang, J. K. Choi, J. Geng, J. W. Jung, S. C. Yoon, and H.-T. Jung, *Small* 5, 2139 (**2009**).
13. J. Bang, K. Kim, S. Mok, F. Ren, S. J. Pearton, K. H. Baik, S. H. Kim, J. Kim, and K. Shin, *Phys. Status Solidi A* 204, 3417 (**2007**).
14. X.-X. Fu, X.-N. Kang, B. Zhang, C. Xiong, X.-Z. Jiang, D.-S. Xu, W.-M. Du, and G.-Y. Zhang, *J. Mater. Chem.* 21, 9576 (**2011**).
15. T. Yanagishita, K. Nishio, and H. Masuda, *Appl. Phys. Express* 2, 022001 (**2009**).
16. K. Choi, S. H. Park, Y. M. Song, Y. T. Lee, C. K. Hwangbo, H. Yang, and H. S. Lee, *Adv. Mater.* 22, 3713 (**2010**).
17. H.-P. Wang, K.-T. Tsai, K.-Y. Lai, T.-C. Wei, Y.-L. Wang, and J.-H. He, *Opt. Express* 20, A94 (**2012**).
18. K.-J. Byeon, J.-Y. Cho, J. Kim, H. Park, and H. Lee, *Opt. Express* 20, 11423 (**2012**).
19. W. Zhou, G. Min, Z. Song, J. Zhang, Y. Liu, and J. Zhang, *Nanotechnology* 21, 205304 (**2010**).
20. H. Sai, H. Fujii, K. Arafune, Y. Ohshita, M. Yamaguchi, Y. Kanamori, and H. Yugami, *Appl. Phys. Lett.* 88, 201116 (**2006**).

21. Y. Kanamori, K. Hane, H. Sai, and H. Yugami, *Appl. Phys. Lett.* 78, 142 **(2001)**.
22. T. Sun, Z. Xu, W. Zhao, X. Wu, S. Liu, Z. Zhang, S. Wang, W. Liu, S. Liu, and J. Peng, *Appl. Surf. Sci.* 276, 363 **(2013)**.
23. N. Koo, U. Plachetka, M. Otto, J. Bolten, J.-H. Jeong, E.-S. Lee, and H. Kurz, *Nanotechnology* 19, 225304 **(2008)**.
24. T. Sun, Z. Xu, S. Wang, W. Zhao, X. Wu, S. Liu, W. Liu, J. Peng, Z. Wang, and X. Zhang, *J. Nanosci. Nanotechnol.* 13, 1871 **(2013)**.
25. M. Beck, M. Graczyk, I. Maximov, E. L. Sarwe, T. G. I. Ling, M. Keil, and L. Montelius, *Microelectron. Eng.* 61–62, 441 **(2002)**.
26. W. Zhou, J. Zhang, X. Li, Y. Liu, G. Min, Z. Song, and J. Zhang, *Appl. Surf. Sci.* 255, 8019 **(2009)**.
27. A. B. D. Cassie and S. Baxter, *Trans. Faraday Soc.* 40, 546 **(1944)**.
28. R. N. Wenzel, *Ind. Eng. Chem.* 28, 988 **(1936)**.
29. H. Park, K.-J. Byeon, K.-Y. Yang, J.-Y. Cho, and H. Lee, *Nanotechnology* 21, 355304 **(2010)**.
30. D. Stavenga, S. Foletti, G. Palasantzas, and K. Arikawa, *P. Roy. Soc. Lond. B Bio.* 273, 661 **(2006)**.
31. C.-T. Wu, F.-H. Ko, and C.-H. Lin, *Appl. Phys. Lett.* 90, 171911 **(2007)**.
32. K. Hadobás, S. Kirsch, A. Carl, M. Acet, and E. Wassermann, *Nanotechnology* 11, 161 **(2000)**.
33. T. Yanagishita, K. Nishio, and H. Masuda, *Appl. Phys. Express* 1, 067004 **(2008)**.
34. S. Grimm, R. Giesa, K. Sklarek, A. Langner, U. Gösele, H.-W. Schmidt, and M. Steinhart, *Nano Lett.* 8, 1954 **(2008)**.
35. P. Zhong, W. Que, and X. Hu, *Appl. Surf. Sci.* 257, 9872 **(2011)**.
36. Z. Wang, T. Sun, L. Wang, Q. Zuo, Y. Zhao, Z. Xu, and W. Liu, *J. Micromech. Microeng.* 22, 125025 **(2012)**.
37. A. F. Feil, P. Migowski, J. Dupont, L. V. Amaral, and S. R. R. Teixeira, *J. Phys. Chem. C* 115, 7621 **(2011)**.
38. N. Yamaguchi, K. Tadanaga, A. Matsuda, T. Minami, and M. Tatsumisago, *Surf. Coat. Tech.* 201, 3653 **(2006)**.
39. C. Chiu, H. Yen, C. Chao, Z. Li, P. Yu, H. Kuo, T. Lu, S. Wang, K. M. Lau, and S. Cheng, *Appl. Phys. Lett.* 93, 081108 **(2008)**.
40. H. Gao, F. Yan, Y. Zhang, J. Li, Y. Zeng, and G. Wang, *J. Phys. D Appl. Phys.* 41, 115106 **(2008)**.
41. T. S. Kustandi, W. W. Loh, H. Gao, and H. Y. Low, *ACS Nano* 4, 2561 **(2010)**.
42. M. Aryal, F. Buyukserin, K. Mielczarek, X.-M. Zhao, J. Gao, A. Zakhidov, and W. Hu, *J. Vac. Sci. Technol. B* 26, 2562 **(2008)**.
43. M. Kokonou, K. Giannakopoulos, and A. Nassiopoulou, *Thin Solid Films* 515, 3602 **(2007)**.
44. O. H. Park, J. Y. Cheng, M. Hart, T. Topuria, P. M. Rice, L. E. Krupp, R. D. Miller, H. Ito, and H. C. Kim, *Adv. Mater.* 20, 738 **(2008)**.
45. A. Li, F. Müller, A. Birner, K. Nielsch, and U. Gösele, *J. Appl. Phys.* 84, 6023 **(1998)**.
46. L. Yi, L. Zhiyuan, C. Shuoshuo, H. Xing, and H. Xinhua, *Chem. Commun.* 46, 309 **(2010)**.
47. S.-W. Ryu, J. Park, J.-K. Oh, D. H. Long, K.-W. Kwon, Y.-H. Kim, J. K. Lee, and J. H. Kim, *Adv. Funct. Mater.* 19, 1650 **(2009)**.

Received: 29 August 2013. Accepted: 9 October 2013.